UHASSELT
KNOWLEDGE IN ACTION

Maastricht University

Faculty of Medicine and Life Sciences
School for Life Sciences
Master of Biomedical Sciences

Master's thesis

GDEPT for oral squamous cell carcinoma: a dental pulp stem cell-based approach

Sara Fieten

Thesis presented in fulfillment of the requirements for the degree of Master of Biomedical Sciences, specialization Molecular Mechanisms in Health and Disease

SUPERVISOR :

Prof. dr. Esther WOLFS

MENTOR :

Mevrouw Jolien VAN DEN BOSCH

2021
2022

Transnational University Limburg is a unique collaboration of two universities in two countries: the University of Hasselt and Maastricht University.

UHASSELT
KNOWLEDGE IN ACTION

www.uhasselt.be
Universiteit Hasselt
Campus Hasselt:
Martelarenlaan 42 | 3500 Hasselt
Campus Diepenbeek:
Agoralaan Gebouw D | 3590 Diepenbeek

Faculty of Medicine and Life Sciences
School for Life Sciences
Master of Biomedical Sciences

Master's thesis

GDEPT for oral squamous cell carcinoma: a dental pulp stem cell-based approach

Sara Fieten

Thesis presented in fulfillment of the requirements for the degree of Master of Biomedical Sciences, specialization Molecular Mechanisms in Health and Disease

SUPERVISOR :

Prof. dr. Esther WOLFS

MENTOR :

Mevrouw Jolien VAN DEN BOSCH

GDEPT for oral squamous cell carcinoma: a dental pulp stem cell-based approach*

Fieten S.[1], Van den Bosch J.[1], Lambrichts I.[1] and Wolfs E.[1]

[1]Cardio & organ systems research group, Biomedical Research Institute, Universiteit Hasselt, Campus Diepenbeek, Agoralaan Gebouw C - B-3590 Diepenbeek

*Running title: A dental stem cell-mediated GDEPT for OSCC

To whom correspondence should be addressed: Prof. dr. Wolfs Esther, Tel: +32 (11) 26 92 96; Email: esther.wolfs@uhasselt.be

Keywords: DPSC, OSCC, The bystander effect, GDEPT, HSV1-tk/GCV

ABSTRACT

Oral squamous cell carcinoma (OSCC) refers to malignancies occurring in the oral cavity. Current therapies cause serious side effects and reduce quality of life. Hence, more targeted and specific treatment is required. We aim to develop dental pulp stem cells (DPSC)-mediated gene-directed enzyme prodrug therapy to eradicate OSCC. Here, the herpes simplex virus type 1–thymidine kinase (HSV1-tk) gene is lentivirally overexpressed in DPSC using a polycistronic construct co-expressing the Firefly luciferase gene, generating HSV1-tk$^+$-DPSC. HSV1-TK enables the cell to convert the prodrug ganciclovir (GCV) into its cytotoxic variant leading to apoptosis. Through gap junctional intercellular communication (GJIC), this cytotoxic GCV is transferred to OSCC cells facilitating cancer cell death. This project confirmed successful lentiviral transduction of DPSC through bioluminescence imaging (BLI), (q)PCR, and ICC. Furthermore, GJIC was confirmed through connexin 43 expression analysis in a 2D and 3D co-culture model and Lucifer Yellow dye transfer. The killing efficiency of HSV1-tk$^+$-DPSC after GCV administration was examined with confluency and alamarBlue analysis. Here, a significant reduction of cell viability was established with a GCV concentration starting from 0.1µM. Lastly, *in vivo* HSV1-tk$^+$-DPSC persistence was assessed with BLI showing a decrease in photon emission after GCV administration, indicating cell death. In conclusion, these results demonstrate the potential of HSV1-tk$^+$-DPSC as a novel targeted therapy for OSCC.

INTRODUCTION

Cancer - Cancer, also called neoplasm or malignant tumor, is a broad group of diseases that can start anywhere in the body (1). This illness progresses with abnormal cells growing uncontrollably, evading their usual boundaries, and eventually spreading to other organs, also called metastasis. The progression from normal cells into uncontrollably growing tumor cells is a multi-stage process resulting from the interaction of one's genetic factors with external carcinogens such as tobacco or ultraviolet light. Various mechanisms for tumor development are compiled in the hallmarks of cancer, where Hanahan D. and Weinberg R.A. were the first to describe them (2). The first hallmarks are self-sufficiency in growth factors, insensitivity to antigrowth signals, evading apoptosis, sustained angiogenesis, tissue invasion and metastasis, and limitless replicative potential. In 2011, four new hallmarks were added: deregulating cellular energetics, avoiding immune destruction, genome instability and mutation, and tumor promoting inflammation (3). The four lastly added hallmarks were recently proposed by Senga S.S. and Grose R.P., namely dedifferentiation and transdifferentiation, epigenetic dysregulation, altered microbiome, and altered neuronal signaling (4).

Head and neck cancer - More than 19 million new cases and almost 10 million deaths accounted for cancer in 2020, making this the second leading cause of death worldwide (5). Of these new cases, 900 000 are attributed to head and neck cancers, with over 400 000 deaths annually around the globe. Head and neck cancers usually start to

develop in the squamous cells lining the mucosal surfaces, referred to as head and neck squamous cell carcinomas (6). Moreover, this cancer type can develop in the pharynx, larynx, nasal cavity, salivary glands, or oral cavity. Over 90% of the lesions in the oral cavity are of the oral squamous cell carcinoma (OSCC) cancer type (7). OSCC refers to lesions formed in the posterior one-third of the tongue, the vermillion border of the lips, and the junction of the hard and soft palates (8). Furthermore, this cancer type occurs as red or white/red lesions, a lump, a non-healing extraction socket, a cervical lymph node enlargement, or an ulcer with fissuring or raised exophytic margins (7). The most prominent risk factors for developing this disease are smoking, alcohol use, and human papillomavirus infections (9-11). The combination of alcohol abuse and heavy smoking, more than two packs a day, is estimated to increase the risk 100-fold for women and 38-fold for men (8).

Current treatment options for oral squamous cell carcinoma - Treatment of OSCC depends on the cancer stage. In most cases, the first treatment option is surgery which can be followed by radiotherapy or chemotherapy in more advanced stages of the disease (12). However, the lesions are initially asymptomatic leading to a diagnosis at a later time point (8). At that time, the lesions are substantially increased, and more extensive parts of the face need to be removed. This causes oral disabilities, such as problems with swallowing, speech, and distortion of the face (8, 12). These issues result in the need for facial reconstruction, and speech and swallowing therapy. Moreover, post-operational radiotherapy and chemotherapy can also result in serious side effects such as loss of taste, open sores, or radiotherapy-induced xerostomia (13-15). Besides these directly induced side effects, radiotherapy also causes late radiation-induced toxicity (16). This refers to side effects emerging more than two months after treatment with radiotherapy such as osteoradionecrosis or long-term percutaneous endoscopic gastrostomy tube dependence. Two other treatment options have been proposed to overcome these severe side effects that follow conventional therapies, namely immunotherapy and targeted therapy. These treatment options are combined with the conventional therapies in the clinical practice but still result in significant side effects and discontinuation of treatment programs (17-19).

Gene therapy – In contrast to the treatments mentioned above, gene therapy is more specific and causes fewer side effects. Here, vectors insert nucleic acids from an exogenous source into target cells to alter gene expression (20, 21). In general, two strategies lie at the basis of gene therapy (21). In the first one, stem cells or precursor cells are transduced with vectors, causing nucleic acid insertion into this cell's DNA. This causes the passage of the exogenous nucleic acid to every daughter cell. In the second basic strategy, a vector is introduced in a slowly dividing or postmitotic cell. With this strategy, the nucleic acid does not integrate into the DNA of this cell, resulting in the expression of the exogenous nucleic acid only for the remaining of that cell's life and not in every daughter cell. The most widely studied gene therapies for cancer are gene-directed enzyme prodrug therapy (GDEPT), immunization gene therapy, and cancer suppressor gene therapy. The latter restores the normal function of cancer suppressor genes, such as p53, through various strategies enabling cell death (20). Immunization gene therapy provides the transfer of exogenous immune system-related genes, such as cytokines or tumor antigens, into the appropriate target cells to improve the anti-tumor immunity.

Gene-directed enzyme prodrug therapy - GDEPT is also called gene prodrug activation therapy or suicide gene therapy. This emerging gene therapy uses transgenes that encode enzymes that are able to convert prodrugs into cytotoxic metabolites, leading to apoptosis of the host cell. The two most widely studied GDEPT are the herpes simplex virus type 1–thymidine kinase (HSV1-tk) ganciclovir (GCV) system (HSV1-tk/GCV) and the cytosine deaminase (CD) 5-fluorocytosine (5-FC) system (CD/5-FC). The latter uses cells containing CD, a bacterial enzyme from *Escherichia coli*, that is able to convert relatively non-toxic 5-FC into 5-fluorouracil (5-FU), a highly chemotherapeutic agent (22). A considerable amount of clinical trials utilizing the CD/5-FC system are in progress. However, reports of these studies are still awaiting. Furthermore, 5-FU can rapidly diffuse out of cells making it less specific and more challenging to report the chemotherapeutic agent in patients (23).

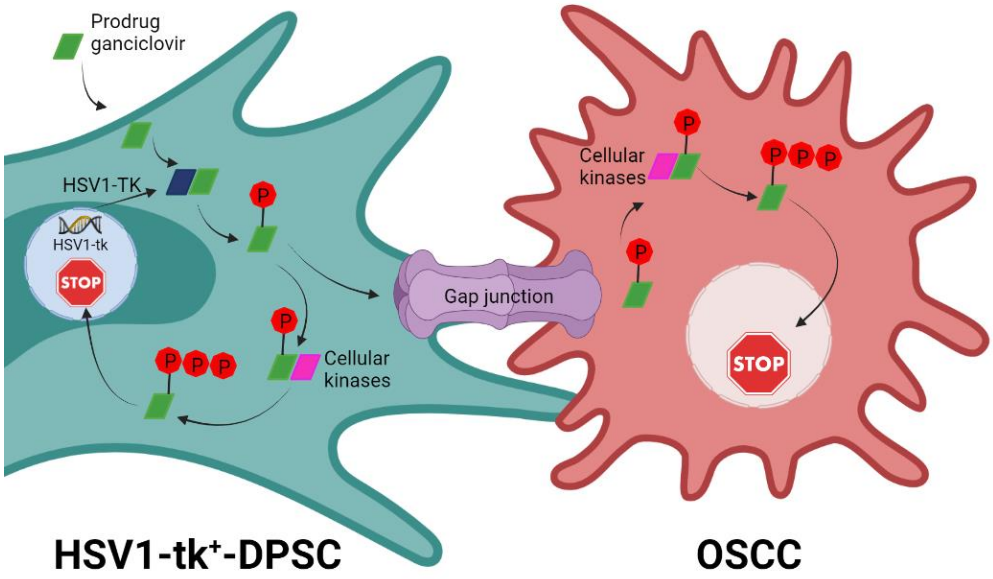

Figure 1: The concept of the bystander killing effect using the HSV1-tk/GCV system. The prodrug ganciclovir (GCV) can diffuse through the cell membrane of the HSV1-tk$^+$-DPSC. Here, GCV will be phosphorylated into GCV monophosphate by HSV1-TK. Its further phosphorylation by cellular kinases leads to the formation of GCV triphosphate, which enters the cell's nucleus and interferes with DNA synthesis. Gap junctions enable its passage to tumor cells, leading to tumor cell death.
HSV1-TK/HSV1-tk: Herpes simplex virus type 1 – thymidine kinase; DPSC: Dental pulp stem cells; OSCC: Oral squamous cell carcinoma
Figure created with biorender.com

The herpes simplex virus type 1-thymidine kinase/ganciclovir system – The second most widely researched suicide gene therapy is the HSV1-tk/GCV system. Here, the prodrug GCV is converted into its toxic metabolite GCV triphosphate after which it is incorporated into the DNA structure. This leads to replication-dependent double-stranded breaks and S and G_2/M arrest (24) (**Figure 1**). Since HSV1-TK has a 1000-fold higher affinity for GCV than the cytosolic human TK, the first phosphorylation step of GCV predominantly occurs through viral TK. (25). Although HSV1-TK has a higher affinity for GCV than its endogenous substrate, a high dosage of GCV is still required for optimal site-targeting leading to off-target toxicity such as bone marrow suppression (25, 26). Therefore, researchers have investigated a way to make HSV1-TK more potent. To this end, the HSV1-sr39tk variant was created through semi-random sequence mutagenesis for an enhanced ability to convert prodrugs, such as GCV, into cytotoxic metabolites (27). Black *et al.* established that even with a 294-fold decrease in GCV dosage, this mutant showed an effect compared to the wild-type HSV1-tk, where no response was observed (28).

In contrast to the CD/5-FC system, phosphorylation of GCV causes entrapment in the cell, making this HSV1-tk based suicide gene therapy more specific (29). Furthermore, HSV1-tk can be visualized through positron emission tomography (PET). Hence, HSV1-tk is also called a PET reporter gene. Three classes of PET reporter genes have been identified: receptor-ligand, ion-transporter, and enzyme-substrate-based systems (30). HSV1-tk belongs to the latter, meaning that it can be visualized using radiolabeled substrates that are nucleoside analogs such as 9-[4-[18F]fluoro-3-(hydroxymethyl)butyl]guanine ([18F]FHBG) (31). These substrates are taken up by cells and phosphorylated if the compatible enzyme HSV1-TK is present. The radiolabeled substrates have a poor affinity for the mammalian thymidine kinase enzyme but a high affinity for HSV1-TK; thus, the radiolabeled substrates will be trapped to a greater extent in HSV1-TK expressing cells. [18F]FHBG, for example, has already been used to visualize adenovirally induced HSV1-tk in hepatocellular

carcinoma of liver cancer patients (32). Additionally, HSV1-tk functions as a safety switch, meaning that genetically manipulated cells will undergo cell death after administration of GCV (23). Hence, these cells can no longer serve as a safety threat.

Therapeutic effects of GDEPT are based on the bystander effect of which there are three types. With the first type, cytotoxic metabolites are encapsulated in apoptotic bodies released from dying genetically manipulated cells. These apoptotic bodies are taken up by neighboring non-transduced cells through endocytosis which causes the release of the cytotoxic metabolite and progression to cell death in the non-transduced cells (25). The second type is also called the distant bystander effect, where immune cells are attracted into the primary tumor site, followed by a systemic immune reaction to the metastatic tumor sites. This mechanism comes from the release of tumor-associated antigens from dying tumor cells, which triggers an anti-tumor response. The last bystander effect type is gap junctional intercellular communication (GJIC), where neighbor non-transduced cells will be provided by the genetically engineered cells with cytotoxic metabolites through the formation of gap junctions. These gap junctions are membrane channels made out of connexin proteins linking the cytoplasm of two neighboring cells enabling the passage of substances such as salts and metabolites (33). Every connexin protein can form homomeric channels with identical isoform proteins or heteromeric hemichannels with distinctive isoform proteins. Connexin 43 (Cx43), named after its molecular weight of 43 kDa, is the most extensively studied connexin protein in humans for GJIC (34). Studies have shown that gap junctions formed out of Cx43 proteins can transfer substances in a wide range up to 760 kDa (35).

The success of the GDEPT depends on the following three components of the system: the inactive prodrug, a gene that codes for an enzyme able to convert the inactive prodrug into an active drug, and a carrier. Until now, suicide gene delivery is mainly executed through viral vectors (25, 36). However, this delivery system has proven to be a suboptimal delivery system concerning safety issues causing severe immune responses, non-specificity, high production costs, and the possibility of insertional mutagenesis (25, 37). Hence, a safer carrier for GDEPT has to be researched.

Stem cells – Stem cells are undifferentiated cells present in the embryonic, fetal, and adult life stages (38). These cells can develop into differentiated cells, becoming building blocks of tissues and organs. Stem cells have three major characteristics: self-renewal which is the ability to proliferate extensively, clonality meaning that they arise from a single cell, and potency which is the ability to differentiate into diverse cell types. However, these properties differ between various stem cell types.

Mesenchymal stem cells (MSC) are plastic adherent cells with an enormous self-renewal capacity. Additionally, these clonogenic cells have a multipotent trilineage differentiation capacity meaning that they can differentiate into chondrogenic, osteogenic, and adipogenic cells (39). In 2005, the Committee of Mesenchymal Stem Cells and Tissues of the International Society for Cellular Therapy (ISCT) suggested that over 95% of the MSC population expresses at least the surface antigens CD90, CD73, CD105 and that MSC are negative (<2%) for hematopoietic and endothelial cell lineage markers such as CD11b or CD45 (40). In addition, MSC possess the remarkable capacity to home to tumor cells meaning that they can be used as vehicles to deliver anti-cancer drugs (41). Furthermore, MSC have immunomodulatory properties enabling them to be administered in an allogeneic setting without evoking an immune response. This leads to fewer side effects upon stem cell administration (42, 43).

Dental pulp stem cells (DPSC) are a subtype of these MSC residing in the perivascular nice of the dental pulp (44). Compared to the bone marrow-derived MSC, these DPSC are less invasive to isolate since they are considered waste products derived from the isolation of wisdom teeth (45). Similar to the MSC, DPSC have a tumor homing capacity. Our research group recently investigated the tumor homing capacity of DPSC towards head and neck cancers (46). This study has shown that DPSC migrate towards tumor cells *in vitro* without significantly influencing the morphology, growth, angiogenesis, and epithelial-to-mesenchymal transition of the head and neck cancers.

Objectives and experimental approach – During this study, lentivirally transduced DPSC encoding the HSV1-tk suicide gene are used as delivery vehicles for the cytotoxic GCV, which is transferred to OSCC cells through GJIC causing cancer cell death (**Figure 1**).

This study aims to validate the successful transduction of DPSC, the presence of functional gap junctions between DPSC and OSCC cells, efficient HSV1-tk$^+$-DPSC cell killing *in vitro* and transduced DPSC persistence *in vivo*. First, successful transduction in three different DPSC donor cell lines will be investigated. To this end, (q)PCR will be performed to measure HSV1-tk mRNA levels, immunocytochemistry (ICC) stainings for protein levels, and bioluminescence imaging (BLI) experiments for the presence of firefly luciferase (Fluc), a gene that is also present in the polycistronic construct inserted in the DPSC donor cell lines. Second, validation of functional gap junction formation between DPSC and OSCC cells will be assessed through immunofluorescent staining of Cx43 proteins in 2D and 3D co-cultures and Lucifer Yellow distribution between the two cell types. Third, the killing efficiency of transduced DPSC will be examined through confluence and alamarBlue analysis. Last, *in vivo* HSV1-tk$^+$-DPSC persistence will be examined by subcutaneous cell injection in mice and followed up with BLI.

We hypothesize that the three DPSC donor cell lines will be successfully transduced and efficiently kill OSCC cells by making functional gap junctions *in vitro*. The results of this study will provide insight into the use of suicide gene therapy with the HSV1-tk/GCV system as a treatment option for OSCC leading to a local, more specific treatment with fewer side effects than the current conventional methods. Additionally, this research will gain information on the functioning of the HSV1-tk/GCV suicide gene therapy and the bystander effect, which will provide insights for further studies on these topics.

EXPERIMENTAL PROCEDURES

Cell isolation and culture – Human DPSC were isolated out of the dental pulp of third molars from healthy donors undergoing tooth extractions for orthodontic or therapeutic reasons with informed consent at Ziekenhuis Oost-Limburg (ZOL). Cells were isolated as previously described (47). Afterward, cells were cultured in alpha modified Minimum Essential Medium (α-MEM, Sigma-Aldrich, St-Louis, MO, USA) enriched with 10% heat-inactivated fetal bovine serum (FBS, Biowest, Nuaillé, France), 2mM L-glutamine, 100U/ml penicillin, and 100µg/ml streptomycin (Sigma-Aldrich, St-Louis, MO, USA). DPSC culture medium was refreshed every 2-3 days. If ~70-80% confluence had been reached, cells were passaged using 0.05% Trypsin/EDTA (Sigma-Aldrich, St-Louis, MO, USA).

The UM-SCC-14C tumor cell line (CLS cell lines service, Eppelheim, Germany, CVCL_7721), a human OSCC cell line, was cultured in Gibco^{TM} DMEM/F12 (Thermo Fisher Scientific, Geel, Belgium) supplemented with 5% heat-inactivated FBS, 100 U/ml penicillin and 100 µg/ml streptomycin.

To distinguish both cell types in 1:1 co-cultures, DPSC and OSCC are colored with ViaFluor® 488 and ViaFluor® 405 cell proliferation kits, respectively (Biotium, Fremont, United States) according to the manufacturer's protocol. Gap junction formation and functionality experiments were performed two days after reaching 100% confluence. Collagen hydrogels were formed out of 10.000 cells/µl mixed with 10% Minimum Essential Medium Eagle (MEM, Sigma-Aldrich, St-Louis, MO, USA) and 80% type 1 rat tail collagen (First Link, Wolverhampton, United Kingdom) (5 mg/ml in 0.6% acetic acid), followed by neutralization with sodium hydroxide.

Lentiviral vector construction, production, and DPSC transduction – DPSC were transduced with a lentiviral vector encoding the EF1α promoter, HSV1-sr39tk, a T2A linker sequence, His-FLAG tagged Fluc, IRES linker sequence, and a puromycin resistance cassette (HSV1-tk$^+$-DPSC) as described by Tiscornia *et al*. (48). Briefly, cells were seeded at $2{,}5x10^3$ cells/cm² in a 24-well plate. Lentiviral particles were added to the cultured DPSC (titer between $5x10^5$ UI/mL and $5x10^7$ UI/mL). The selection of transduced DPSC was based on puromycin resistance after seven days (1 µg/ml, #ant-pr-1, InvivoGen, Toulouse, France).

RNA isolation, cDNA production, and (quantitative) Polymerase chain reaction ((q)PCR) – $35x10^3$ DPSC/cm^2 were seeded in 24-well plates. After reaching 80% confluence, total RNA was

isolated with the TRIzol™ reagent (Invitrogen, Thermo Scientific, Geel, Belgium) method using QIAzol (Qiagen Sciences, Venlo, The Netherlands) according to the manufacturer's instructions. RNA quality was evaluated using NanoDrop 2000c Spectrophotometer (Thermo Fisher Scientific, Geel, Belgium). 1 ng/µl cDNA was synthesized using qScript® cDNA SuperMix (Quantabio, Leuven, Belgium) according to the manufacturer's protocol. For PCR, cDNA was amplified with the KAPA Mouse Genotyping Kit (Sigma-Aldrich, St-Louis, MO, USA) according to the manufacturer's protocol except for the cycling protocol being: 30x(95°C for 1 min, 95°C for 30 sec, 59.5°C for 30 sec, 72°C for 1 min), 75°C for 5 min, 4°C for ∞. 505 base pair gel bands were visualized in a 1% agarose gel. Primer pairs (**Table S.2**) and SYBR Green (Applied Biosystems, Thermo Fisher Scientific, Geel, Belgium) were added to cDNA samples for qPCR. Ct values were obtained by Quant Studio (Applied Biosystems, Thermo Fisher Scientific, Geel, Belgium) with the following protocol: 95°C for 20 sec, 40x(95°C for 3 sec, 60°C for 30 sec), 95°C for 15 sec, 60°C for 60 sec, 95°C for 15 sec. Primer pair efficiencies were tested.

In vitro bioluminescence imaging (BLI) – $10x10^3$ cells/cm^2 were seeded on black/clear bottom 96-well plates. According to the manufacturer's instructions, the Fluc activity was measured via the OneGlo™ Luciferase Assay System (Promega, Leiden, The Netherlands) and analyzed with the CLARIOstar® PLUS plate reader (BMGLABTECH, De Meern, The Netherlands).

Immunocytochemistry (ICC) analysis – $35x10^3$ cells/cm^2 were seeded on glass coverslips in a 24-well plate. Cells or hydrogels were fixated with Unifix (VWRK4031-9010, Klinipath, Olen, Belgium) for 20 or 40 min, respectively, at room temperature. DPSC were permeabilized with 0.05% Triton X-100 diluted in PBS for 30 min at 4°C when required for intracellular visualization. Next, cells or hydrogels were treated with a protein blocker for one or three hour(s), respectively, at room temperature to block non-specific binding sites. For immunofluorescence, cells were incubated overnight at 4°C in primary anti-His, FLAG, HSV1-TK, or Cx43 (**Table S.3**). Primary antibodies for hydrogels were first incubated one hour at room temperature before overnight incubation at 4°C. After thorough rinsing with PBS, cells or hydrogels were incubated for two or six hours, respectively, at room temperature in the dark with secondary antibodies anti-rabbit or anti-mouse (**Table S.3**). Negative control samples lacking primary antibodies were included. Cellular nuclei were counterstained with 4,6-diamidino-2-phenylindole (DAPI) for 30 min at room temperature in the dark if nuclear visualization was preferred. Coverslips were mounted with fluoro-mount, and pictures were taken at a magnification of 40x with the Leica DM4000 B microscope (Leica Microsystems, Wetzlar, Germany) for His, FLAG, or HSV1-TK visualization or with the Confocal Zeiss LSM 880 (Zeiss, Zaventem, Belgium) for Cx43 detection.

Lucifer Yellow dye transfer – Functional gap junction formation was assessed through a Lucifer Yellow dye transfer assay. A DPSC/OSCC cell co-culture was seeded in a 35 mm glass-bottom dish (MatTek corporations, Ashland, United States). Two days after reaching 100% confluence, one single DPSC cell was microinjected with 1 mg/ml Lucifer Yellow dye (428/536nm, Sigma-Aldrich, St-Louis, MO, USA L0144). Transfer of the dye was monitored with the ELYRA super-resolution microscope (Zeiss, Zaventem, Belgium) by making a snapshot every other 30s at a magnification of 40x.

Cell viability assays – $10x10^3$ cells/cm^2 of DPSC and OSCC cells were seeded in a 1:1 ratio in a 96-well plate. Two days after reaching 100% confluence, analysis of confluency of the co-culture was assessed over six days with different GCV concentrations (0.01-0.1-1-10-100µM) through live-cell imaging with the Incucyte® live cell analysis (Sartorius, Goettingen, Germany). On day six, alamarBlue (Invitrogen, Thermo Fisher Scientific, Geel, Belgium) was added in a 1/10 ratio to the wells. After 4 hours of incubation, fluorescence was measured with the CLARIOstar® PLUS plate reader (BMGLABTECH, De Meern, The Netherlands).

In vivo HSV1-tk$^+$-DPSC persistence – $50x10^4$ HSV1-tk$^+$-DPSC were resuspended in 25 µl serum-free DMEM medium and 25 µl of growth factor-reduced Matrigel (Corning, Lasne, Belgium) before subcutaneous injection in nude

Hsd:Athymic-*Foxn1*^{nu} mice (Envigo, Horst, The Netherlands). Potential GCV administration was intraperitoneally injected every day at 50 mg/kg. Persistence was followed up by BLI. Mice were anesthetized with isoflurane (2% in 100% oxygen at a flow rate of 2 l/min), after which D-luciferin (Promega, Leiden, The Netherlands) was injected at 126 mg/kg subcutaneously. Photon emission was measured where consecutive frames were received using IVIS lumina III (Perkin Elmer, Mechelen, Belgium) until maximum signal intensity was achieved. Regions of interest (ROI) were marked, and total photon flux of the ROI were quantified.

Statistical analysis – Statistical analysis was carried out using GraphPad Prism 9. Normal distribution of the data was investigated with the Shapiro-Wilk Test. Significant outliers were detected with GraphPad and excluded for analysis. For overexpression determination, a one-sample t-test was performed with a hypothetic value of zero. Significance of cell viability was assessed through one-way ANOVA combined with the Dunnett's multiple comparison test. All data is represented as mean ± standard error of the mean (S.E.M.). Significance levels are indicated as $*p \leq 0.05$, $**p \leq 0.01$, $***p \leq 0.001$, $****p \leq 0.0001$.

RESULTS

This project aimed to validate successful lentiviral transduction of DPSC, confirm the presence of functional gap junctions between DPSC and OSCC cells, evaluate the killing efficiency of the HSV1-tk^{+}-DPSC, and monitor transduced DPSC persistence *in vivo*.

Successful lentiviral transduction of DPSC

To lentivirally overexpress HSV1-tk in DPSC, a polycistronic construct co-expressing imaging reporter gene firefly luciferase (Fluc) was generated (**Figure S.1**). The human elongation factor-1 alpha (EF1α) functions as the promoter which drives the expression of HSV1-tk coupled to a His-FLAG-tagged Fluc and a puromycin resistance cassette. These genes are connected through linker sequences peptide2A (T2A) and the internal ribosome entry site (IRES).

mRNA expression of HSV1-tk in transduced DPSC

To evaluate successful lentiviral transduction of DPSC, mRNA expression of HSV1-tk was assessed through qPCR. The HSV1-tk mRNA levels were normalized to mRNA levels of housekeeping genes tyrosine 3-Monooxygenase/tryptophan 5-monooxygenase activation protein zeta (YWHAZ) and D-serine/alanine/glycine/:H(+)symporter (cycA). **Figure 2.A** shows significant overexpression of HSV1-tk in all three DPSC donor cell lines. The presence of HSV1-tk was further validated through PCR and band visualization on agarose gel electrophoresis, as shown in **Figure 2.B.**

Protein expression of HIS, FLAG, and HSV1-TK in transduced DPSC

Successful lentiviral transduction of DPSC was further confirmed through HIS, FLAG, and HSV1-TK protein expression visualization and quantification through ICC and integrated density analysis. **Figure 2.D** depicts representative images for the three DPSC donor cell lines where HSV1-tk transduced cells stained positive for all three markers (HIS, FLAG, and HSV1-TK) compared to wild-type DPSC lacking marker expression. Controls without primary antibody incubation were included, which showed no marker expression (data not shown). This indicates that there is no non-specific binding of secondary antibodies to the expressed markers. **Figure 2.C** depicts the quantification of the protein expression of the three markers (HIS, FLAG, and HSV1-TK). For all DPSC donor cell lines, there is an elevated trend of the three proteins. However, only the HIS and HSV1-TK markers were significantly overexpressed in P180 and P121.

Photon emission measurement in transduced DPSC

For HSV1-tk expression in DPSC, a polycistronic construct co-expressing Fluc was implemented. Fluc converts substrate D-luciferin into oxyluciferin resulting in measurable photon emission. **Figure 2.E** demonstrates the relative light units (RLU) for the three transduced DPSC cell lines. Every donor cell line presented a significant overexpression of the RLU and thus the expression of Fluc.

These results indicate the successful lentiviral transduction of three DPSC donor cell lines (P165, P180, and P121).

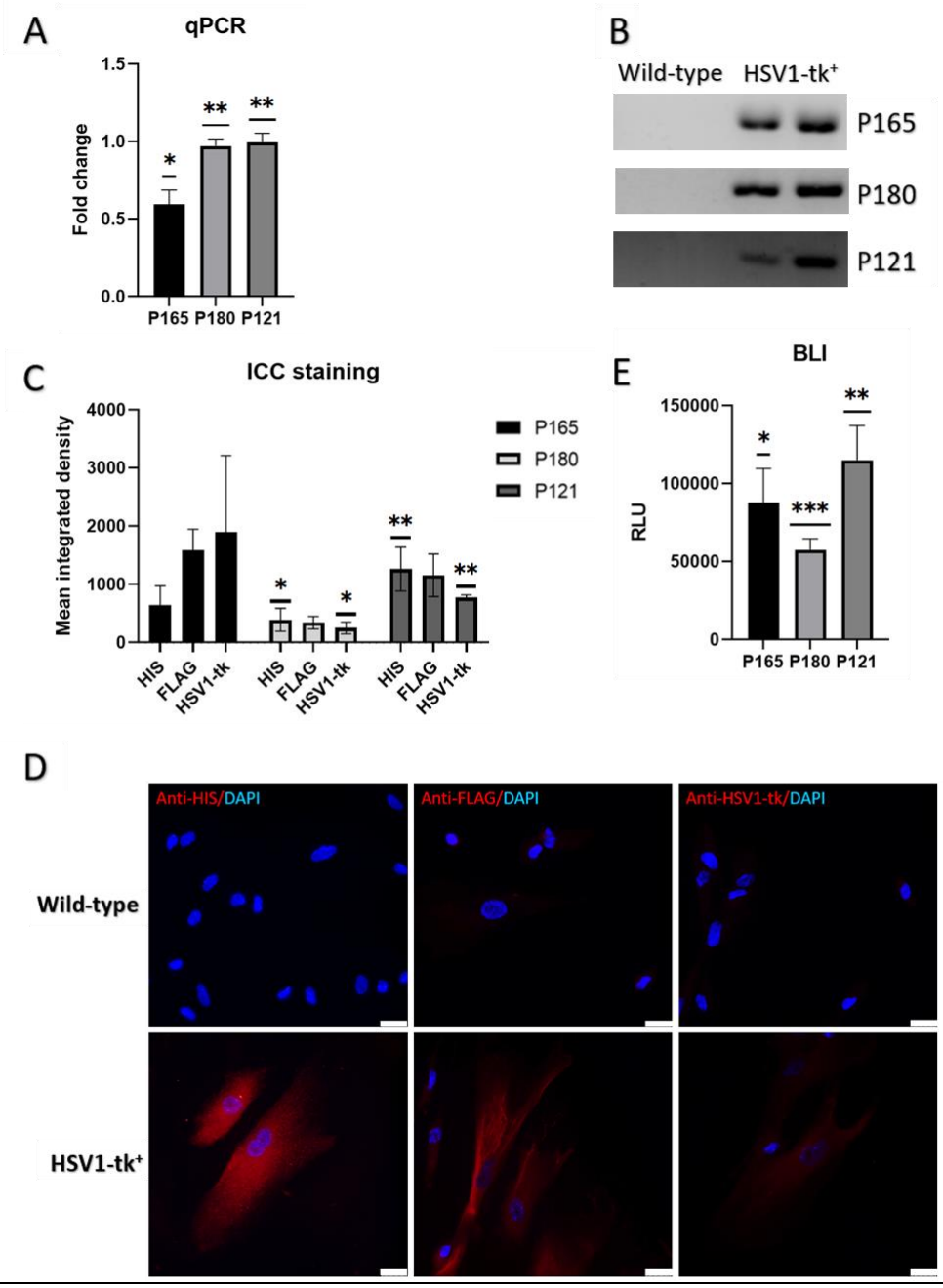

Figure 2 – **Assessment of successful lentiviral transduction in three DPSC donor cell lines.** (**A**) Fold change of HSV1-tk mRNA expression in transduced DPSC assessed through qPCR shows significant overexpression of HSV1-tk mRNA in all three DPSC donor cell lines. N=3 with three technical replicates. (**B**) HSV1-tk gel band visualization is present in transduced DPSC while being absent in wild-type DPSC. N=3 with three technical replicates. (**C**) Quantification of ICC analysis of HIS, FLAG & HSV1-TK shows overexpression of the three markers where HIS and HSV1-TK from P180 and P121 are significant. N=3. (**D**) Representative images obtained with the DM 4000 Fluorescent Microscope (LEICA) at 40x show the presence of the three markers (HIS, FLAG, HSV1-TK) in transduced DPSC while absent in wild-type DPSC. N=3, scale bar=25µm. (**E**) Photon emission obtained from the conversion of D-luciferin into oxyluciferin by Fluc shows significant photon emission overexpression in all three DPSC donor cell lines. N=6 for P165 and P180, N=7 for P121. For all DPSC donor cell lines, three technical replicates were included. All data shown as Mean±S.E.M. A one-sample t-test was performed with a hypothetic value of zero *(*$p \leq 0.05$, **$p \leq 0.01$, ***$p \leq 0.001$).*

ICC: Immunocytochemistry,; BLI: Bioluminescence imaging; HSV1-TK: Herpes simplex virus type 1-thymidine kinase

Preservation of DPSC markers after transduction

To investigate whether transduction influences DPSC integrity, the mRNA levels of CD90, CD73, and CD105 were validated for both wild-type and transduced DPSC of one DPSC donor cell line through qPCR. The mRNA levels were normalized to mRNA levels of housekeeping genes YWHAZ and cycA. **Figure 3** shows that DPSC markers CD90, CD73, and CD105 are expressed in equal amounts on both transduced and non-transduced DPSC. This indicates that transduction does not influence DPSC integrity.

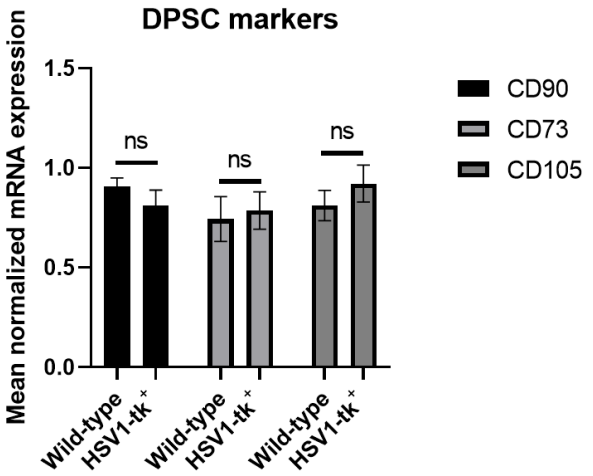

Figure 3 – **DPSC marker expression.** CD90, CD73, and CD105 mRNA is evenly expressed in wild-type and transduced DPSC. N=3 with three technical replicates. A T-test was performed. *ns: Not significant; CD90: Cluster of Differentiation 90; CD73: Ecto-5'-nucleotidase; CD105: Endoglin*

Functional gap junction formation in a DPSC/OSCC co-culture model

Functional gap junction formation is essential to guarantee the bystander effect and transfer of the cytotoxic GCV to OSCC cells causing tumor cell death.

Membrane expression of connexin 43 in a DPSC/OSCC co-culture model

Cx43 expression indicates the formation of gap junctions between adjacent cells. To this end, ICC staining of Cx43 was performed in a co-culture model where cytoplasmic staining can distinguish OSCC cells (blue) and DPSC (green). As revealed in **Figure 4.A**, Cx43 (red) is present on the membranes of both cell types. **Figure 4.B** visualizes a more detailed image of the DPSC/OSCC co-culture. The white arrow demonstrates Cx43 expression at neighboring plasma membranes, indicating gap junction formation between both cells.

To obtain a more representative image of the *in vivo* situation, ICC staining of Cx43 was performed on a stained co-culture model in a collagen hydrogel. **Figure 4.C** confirms that Cx43 is present on the membranes of both cell types when cells are in an *in vivo* representing environment. **Figure 4.D** depicts the connection between DPSC and OSCC cells in more detail. In different layers of the collagen hydrogel, Cx43 expression is observed over the whole edge of these adjacent cells (white arrows), indicating gap junction formation in this 3D model.

Functionality of the formed gap junctions in a DPSC/OSCC co-culture model

Although Cx43 expression indicates the presence of gap junctions, their functionality has to be validated. Therefore, Lucifer Yellow dye transfer analysis was performed in a ViaFluor® stained DPSC/OSCC co-culture model. During this experiment, single-cell microinjection of DPSC with Lucifer Yellow lead to transfer of the dye to neighboring DPSC and OSCC cells (white arrows) over a time period of 25 minutes, validating the functionality of gap junctions formed in these co-cultures (**Figure 5**).

These results validate that functional gap junctions are formed between DPSC and OSCC cells, demonstrating gap-junctional intercellular communication in the *in vitro* model.

Killing efficiency of transduced DPSC in a DPSC/OSCC co-culture model with different GCV concentrations

Cx43 presence and efficient transfer of Lucifer Yellow Dye indicate GJIC. As explained earlier, this means that a proper transfer of the cytotoxic GCV to cancer cells is expected. However, the cell-killing ability of HSV1-tk$^+$-DPSC still has to be validated. To this end, DPSC/OSCC cells were seeded in a 1:1 ratio, and GCV (0.01-0.1-1-10-100 µM) was administered for six consecutive days with fresh medium replacements every 48 hours. Cell viability was investigated through confluency analysis which was validated through an

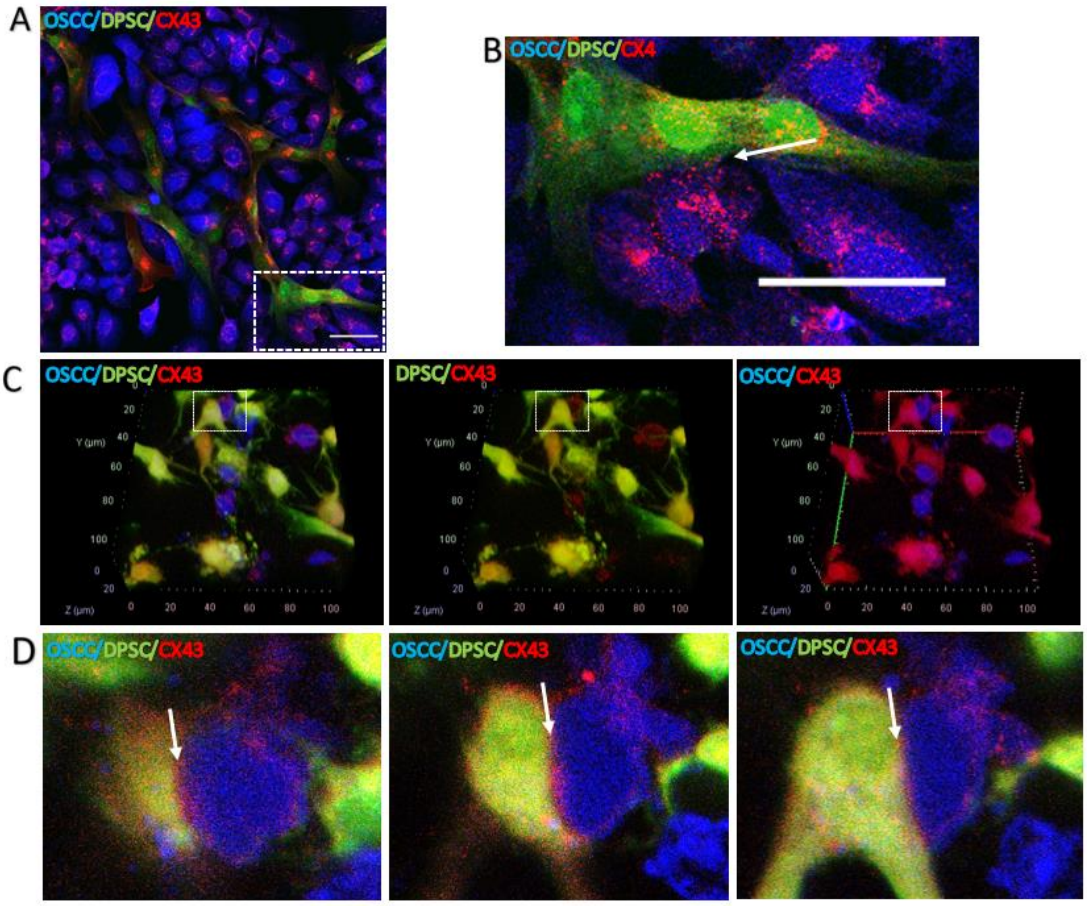

Figure 4 – **Cx43 membrane expression in a 2D and 3D DPSC/OSCC co-culture model.** (**A**) Cx43 (red) membrane expression in a 2D DPSC/OSCC (green/blue) co-culture model distinguished by cytoplasmic dye staining confirmed through ICC analysis. N=3, Scale bar=50µm. (**B**) Magnification of white square in (A) depicts DPSC and OSCC cells neighboring each other with Cx43 membrane expression indication gap junction formation (white arrow). Scale bar=50µm. (**C**) A 3D ViaFluor® stained DPSC/OSCC (green/blue) co-culture in a collagen hydrogel with Cx43 (red) membrane expression on both cell types. (**D**) Magnification of white square in (C) showing Cx43 membrane expression for cells laying in proximity of each other in different planes of the collagen hydrogel, indicating gap junction formation (white arrow). Images were taken at 40x with the Confocal Zeiss LSM 880.
OSCC: Oral squamous cell carcinoma; DPSC: Dental pulp stem cells; Cx43: Connexin 43

alamarBlue assay on day six. **Figure 6.A** depicts the confluency of transduced and wild-type DPSC in co-culture with OSCC cells over six days after GCV administration. 1-10-100 µM concentrations of GCV displayed a reduction in transduced DPSC co-culture confluence starting from day four. On day six, there was a significant reduction in cell confluence of the HSV1-tk^{+}-DPSC co-culture with 1-10-100 µM of GCV treatment (53.53 ± 1.57% (1 µM), 41.09 ± 2.34% (10 µM), 24.97 ± 3.23% (100 µM)) (**Figure 6.B)**. Complementary, alamarBlue analysis also showed a significantly lower cell viability with a GCV concentration of 0.1 µM six days after the start of administration (67.55 ± 1.01%) (**Figure 6.B**). The wild-type DPSC co-culture presented a decrease in confluence after GCV administration of 100 µM (**Figure 6.A**). This cytotoxic effect on non-transduced co-cultures was confirmed on day six with a significant reduction in confluence (47.57 ± 8.46%) and cell viability (75.68 ± 3.13%) as analyzed through confluency and alamarBlue analysis, respectively (**Figure 6.B**). These data indicate the toxicity of high doses of this prodrug.

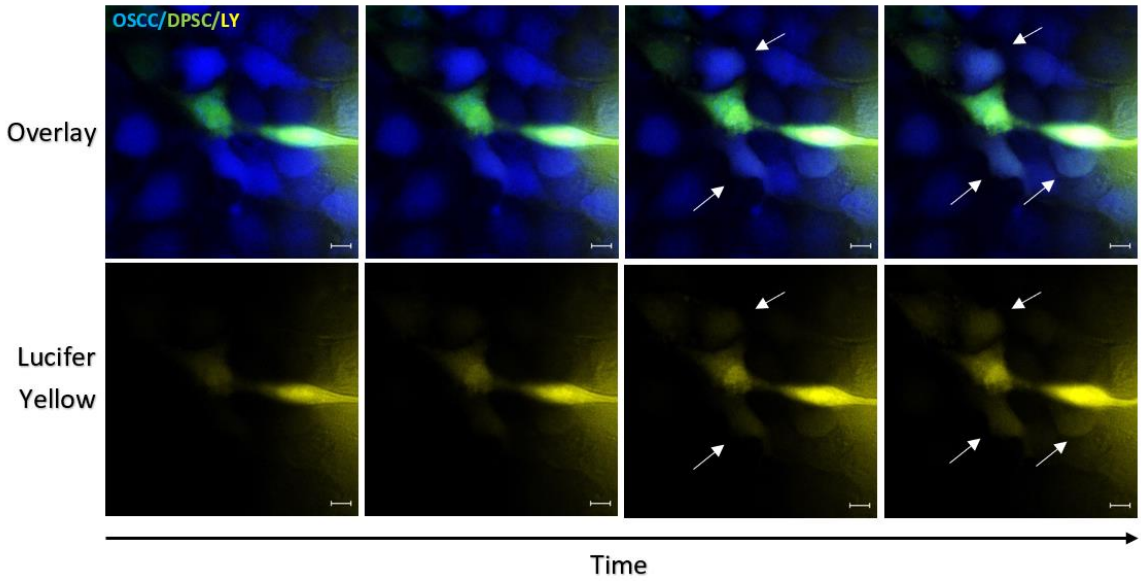

Figure 5 – **Functional gap junction formation in a DPSC/OSCC co-culture model.** Microinjection of one DPSC (green) with Lucifer Yellow dye (428/536 nm) results in the transfer of the dye between DPSC and towards OSCC cells (blue) as imaged in a time-series of 25 minutes with the ELYRA super-resolution microscope at 40x. White arrows indicate Lucifer Yellow dye transfer towards OSCC cells. N=3, scale bar=10µm.
OSCC: Oral squamous cell carcinoma; DPSC: Dental pulp stem cells; LY: Lucifer Yellow

These results indicate the highly efficient cell killing capacity of HSV1-tk$^+$-DPSC starting with a GCV treatment concentration of as low as 0.1 µM. However, the toxicity of high doses of GCV (100 µM) should be considered in further research experiments.

HSV1-tk$^+$-DPSC persistence *in vivo*.

The *in vivo* persistence of transduced DPSC was assessed through BLI. Since Fluc is present in the polycistronic construct inserted in the DPSC, photon emission represents the amount of viable cells that are present. Photon expression was acquired over a time period of 14 days in daily-injected mice receiving GCV and non-injected controls. A reduction in cell viability was obtained with GCV administration after seven days (74.76 ± 15.97% (day 3) vs 15.35 ± 6.03% (day 7)) while the amount of viable cells remained relatively stable in the control group (**Figure 7.A**). Representative images of photon expression measured after GCV administration compared to non-injected controls on day 0-3-7 confirm these results (**Figure 7.B**).

These data indicate the stable survival of HSV1-tk$^+$-DPSC *in vivo*. Seven days after GCV administration, a substantial decrease in cell viability was observed which further confirms the killing efficiency of transduced DPSC.

DISCUSSION

The most common head and neck cancer type, OSCC, has a low 5-year survival rate (49). Conventional therapies, such as chemotherapy and radiotherapy, lack effectiveness and cause severe side effects. Hence, more targeted treatment options are required to reduce the disease burden and treat OSCC. Several preclinical studies show promising results for using HSV1-tk/GCV suicide gene therapy to eradicate numerous cancer types (50-52). However, these studies use viral vectors to deliver HSV1-tk, which is known for its safety issues such as insertional mutagenesis, non-specificity, high costs, and severe immune responses (25). Despite research progression and the production of non-viral alternatives to deliver HSV1-tk to tumor cells, the transfer efficiency remains low (53-55). Recently, stem cells have been suggested as therapeutic carriers for cancer eradication. To this end, stem cells are transduced with the HSV1-tk gene and delivered to the cancer cells. This gene enables the cells to efficiently converse the prodrug GCV into its cytotoxic variant which is transferred

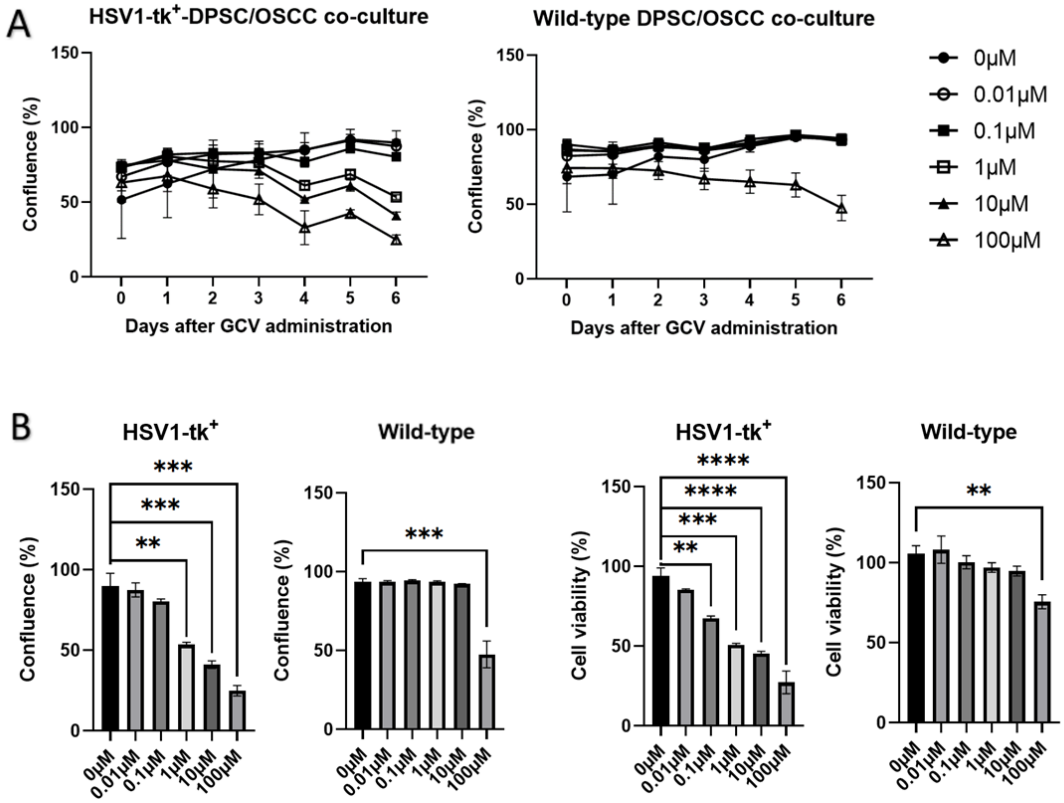

Figure 6 – Cell viability over six days after GCV administration. DPSC/OSCC co-cultures received GCV treatment (0.01-0.1-1-10-100 μM) over six days. An alamarBlue analysis was performed on the last day to determine cell viability. (**A**) The confluence of transduced (HSV1-tk$^+$) and wild-type DPSC in co-culture with OSCC cells over six days after GCV administration. Lower HSV1-tk$^+$-DPSC/OSCC co-culture confluency with 1-10-100 μM of GCV administration indicates cell death. Wild-type DPSC/OSCC co-cultures also showed lower confluence with 100 μM GCV administration, indicating toxicity. (**B**) Percentages of viable cell in co-cultures after confluence (left) or alamarBlue (right) analysis on day six after GCV treatment. Both analyses showed significantly lower HSV1-tk$^+$-DPSC/OSCC co-culture viability with 1-10-100 μM GCV treatment. alamarBlue analysis also demonstrated a significant reduction in viability of this co-culture group with 0.1 μM GCV. Wild-type DPSC/OSCC co-cultures presented significantly less viability with 100 μM GCV, further validating this toxicity. All data is shown as Mean±S.E.M. N=2 with three technical replicates. A one-way ANOVA combined with the Dunnett's multiple comparison test was performed *(**p ≤0.01, ***p ≤0.001, **** p ≤0.0001).*
HSV1-tk: Herpes simplex virus type 1-thymidine kinase; GCV: Ganciclovir

through the bystander effect to the tumor cells causing eradication of the cancer cells (56-58). Therefore, this project aimed to develop DPSC-mediated GDEPT as a novel treatment for OSCC. DPSC are isolated from the dental pulp of third molars donated by healthy volunteers undergoing tooth extractions for orthodontic or therapeutic reasons, meaning that the teeth are considered as waste products. Moreover, DPSC have the advantage of homing toward cancerous tissue, implying that they will specifically target cancer cells which spares healthy tissue (41, 59, 60). In addition, because of the immunomodulatory phenotype of DPSC, no immune response is expected upon administration of this therapy. This means that side effects caused by therapy administration are limited (42, 43).

As a first objective, successful lentiviral transduction of the three DPSC donor cell lines was assessed through (q)PCR, ICC analysis, and BLI. As earlier mentioned, a variant of HSV1-tk created by Black *et al.* called HSV1-sr39tk was used during this project (61). This variant was obtained through

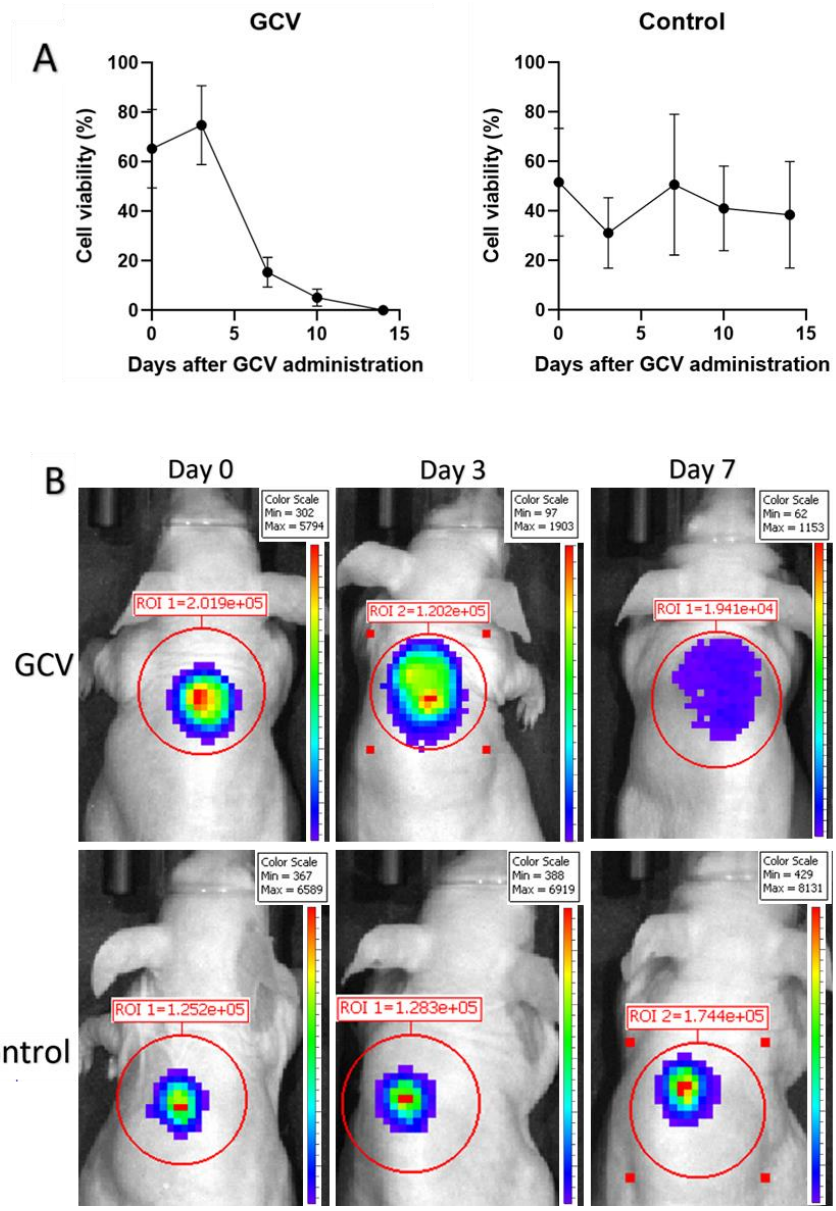

Figure 7 – HSV1-tk$^+$-DPSC persistence *in vivo*. (**A**) Cell viability of transduced DPSC over a time period of 14 days after GCV administration (left) compared to non-injected control animals (right) demonstrated a decrease in cell viability on day 7 with GCV administration while cell viability remained relatively stable in non-injected controls. (**B**) Representative images of photon measurement in mice on day 0-3-7 after GCV administration or no injection (control). Photon signal decreased on day 7 with GCV treatment while remaining relatively stable within the control. N=6 for GCV administration, N=4 for non-injected controls. Data is represented as Mean±S.E.M. Images were taken with the IVIS Lumina III (Perkin Elmer).
GCV: Ganciclovir

semi-random sequence mutagenesis and shows a higher affinity for GCV than wild-type HSV1-tk (28, 62). Furthermore, Gambhir *et al.* showed an increased accumulation of radioactively labeled substrates and so a higher imaging sensitivity of HSV1-sr39tk for PET imaging compared to the wild-type HSV1-tk. This means that this HSV1-tk variant transduced in the stem cells can be tracked more efficiently during PET scanning. Our results demonstrate that all three DPSC donor cell lines

significantly overexpress HSV1-tk mRNA. This indicates the successful transduction of DPSC. However, to examine if this HSV1-tk mRNA is also converted into proteins an ICC analysis was performed. An elevated trend in HSV1-tk protein expression was established which was significant for P180 and P121. This further indicates that we successfully transduced the DPSC donor cell lines. Through the presence of Fluc in the lentiviral vector construct, substrate D-luciferin can be catalyzed into oxyluciferin when ATP and oxygen are present, causing photon emission (63). Fluc has been widely used to non-invasively monitor cells in an *in vivo* setting (64-66). Besides Fluc, other luciferase genes are also used for *in vivo* cell monitoring, such as Renilla luciferase (Rluc). One advantage of using Fluc over Rluc is its capacity to only visualize live cells since Rluc does not require the presence of ATP for substrate catalyzation (63, 67). Our data depicts that photon emission is significantly overexpressed in transduced DPSC, which confirms the presence of Fluc in these transduced stem cells. Overall, these results demonstrate that we successfully transduced three DPSC donor cell lines causing the expression of HSV1-tk. Limited interdonor variability is depicted which can be attributed to a difference in multiplicity of infection (MOI). Factors such as the inconsistent length of vector adsorption and the divergent amount of target cells could influence the transduction efficiency meaning that the number of transduced cells could differ between the patients causing variation in our results (68).

Furthermore, DPSC marker expression after transduction was examined through qPCR analysis. The ISCT classifies three surface markers to be present on DPSC: CD90, CD73, and CD105 (40). mRNA expression of these markers did not change in transduced compared to the wild-type DPSC meaning that transduction does not affect DPSC integrity.

Successful transduction and HSV1-TK expression in DPSC results in cytotoxic GCV production (58). However, the transfer of this cytotoxic metabolite to the cancer cells still had to be validated. To this end, functional gap junction formation between DPSC and OSCC cells *in vitro* was examined as the second objective. Gap junctions are formed out of connexons which are hexamers of connexin proteins (34). There are 21 human isoforms of this protein, of which Cx43 is the most widely studied. The presence of this protein in cell membranes indicates the formation of gap junctions. Cx43 expression on OSCC cells was already demonstrated earlier at protein and mRNA levels (69-71). Brockmeyer *et al.* showed that Cx43 mRNA expression is significantly upregulated in OSCC compared to normal oral squamous tissue (70). In addition, this group researched that high Cx43 membrane expression is a significant independent prognostic marker for a short overall survival length (71). This suggests that Cx43 membrane expression may promote the formation of gap junctions with prognostic relevance. Some studies also validated Cx43 mRNA expression and its presence on the membrane of DPSC (72, 73). Our data confirms this membrane expression in DPSC and OSCC cells both in 2D and 3D co-cultures. DPSC/OSCC cell co-cultures were placed in a type 1 collagen hydrogel to give a better representation of the *in vivo* situation (74). Type 1 collagen is the most widely prevalent collagen form in the natural extracellular matrix making this collagen hydrogel a highly used scaffold for 3D analysis.

Although Cx43 presence indicates the formation of gap junctions, their functionality still had to be validated. There are many different techniques to study GJIC. However, microinjection of Lucifer Yellow has several advantages (75). This technique allows for evaluating the transfer rate from one cell to another because of the accurately controlled duration of Lucifer Yellow dye injection. Furthermore, morphological and functional data of individual cells can be correlated because of the selective dye loading of one cell. In addition, cell communication between different cell types can be compared since the level of communication is expressed as the amount of dye-coupled cells. The functionality of gap junctions between stem cells and cancer cells has been established in research through various techniques (56). Conform with these findings, our results demonstrate Lucifer Yellow dye transfer to neighboring DPSC and OSCC cells after single-cell microinjection of DPSC. These data suggest that functional gap junctions are formed in DPSC/OSCC co-cultures, making GJIC possible to transfer cytotoxic GCV for cancer eradication.

Functional gap junction formation indicates the efficient transfer of cytotoxic GCV from the DPSC to the cancer cells. However, the killing efficiency of the transduced DPSC had to be confirmed. As a third objective, this HSV1-tk$^+$-DPSC killing efficiency and the optimal GCV concentration to cause OSCC cell eradication over time were researched. To this end, five concentrations of GCV (0.01-0.1-1-10-100 µM) were added to 1:1 ratios of DPSC/OSCC co-cultures for six executive days. In line with our results, studies using the same GCV concentration range on transduced cancer cells demonstrate a reduction of cell viability starting from a GCV concentration as low as 0.1 µM (76, 77). A concentration of 100 µM showed a decrease of non-transduced tumor cell viability, indicating toxicity of high doses of GCV. Nonetheless, several studies suggest using even higher concentrations ranging from 200-10,000 µM (62, 78) while a toxic effect was observed on non-transduced cells starting from GCV concentrations of 40 µM, which sharply increased with even higher concentrations. This is conform with our results where a significant reduction in non-transduced co-culture cell viability was observed with 100 µM of GCV. The toxicity of GCV is widely known and has already been demonstrated in patients with Human cytomegalovirus infection undergoing GCV treatment as hematological toxicities such as neutropenia and myelosuppressive effects (79, 80).

However, the studies mentioned above directly transduce tumor cells, while this project uses genetically manipulated stem cells to deliver the toxic GCV variant and eradicate tumor cells. Similar to our research, the study of Matuskova *et al*. uses HSV1-tk transduced MSC to eradicate glioblastoma (56). During this project, transduced stem cell viability was diminished starting from a concentration of 1 µM. Additionally, our results demonstrated a reduction of HSV1-tk$^+$-DPSC co-culture viability starting from a concentration as low as 0.1 µM of GCV. In contrast to our data, a reduction in wild-type MSC was observed after a concentration of 1000 µM while the cells remained viable at 100 µM. These differences can be attributed to using the more potent HSV1-sr39tk variant during our project, while another HSV1-tk variant was used in the project of Matuskova *et al.* Additionally, this study demonstrated that sensitivity to cell death in transduced co-cultures and GCV cytotoxicity in non-transduced co-cultures depended on the cancer cell line that was used. This research group hypothesized that variations between cancer cell lines are most likely due to differences in cell-intrinsic tumor cell properties.

As the last objective, the HSV1-tk$^+$-DPSC persistence was monitored *in vivo*. During this project, mice were injected daily with a GCV concentration of 50 mg/kg. Nonetheless, some studies use much lower concentrations of 10 mg/kg GCV with efficient tumor reduction seven days after the start of treatment (77, 81). Higher concentrations of 100mg/kg GCV successfully demonstrated a tumor reduction as early as five days after starting GCV injections (62, 78, 82). However, during these studies, the HSV1-tk gene was directly transduced in tumor cells. Similar to our objectives, Leten *et al.* used HSV1-tk transduced MSC as vehicles for suicide gene therapy in malignant brain tumors (58). During this study, a daily GCV concentration of 50mg/kg was administered for 14 consecutive days. Their results show that stem cell survival diminished seven days after GCV and PBS injection. This decline is also seen in our results for the GCV treatment group. In contrast, the non-injected control group in our project had a relatively stable cell survival. This can be due to the fact that our project used no injection as a control group compared to PBS injections in the study of Leten *et al.* Furthermore the small sample size (N=4) and relatively large variation in photon expression in our control group can contribute to these varying results.

The data of this project shows great promise in using HSV1-tk expressing DPSC as therapeutic vehicles to eradicate OSCC. However, further research is necessary to strengthen these results. As a primary future perspective, there should be focused on the examination of DPSC marker expression after transduction. During this project, marker expression was only investigated for one of the DPSC donor cell lines, while this should be confirmed in all of them. Furthermore, only the expression of markers present on DPSC was investigated even though the ISCT specifies the absence of hematopoietic and endothelial cell linage markers (40). In Addition, not only mRNA expression but also cell surface expression of these

markers should be examined since mRNA production does not guarantee translocation to the membrane.

Although functional gap junction formation was demonstrated during this project, further research is needed to confirm this GJIC in DPSC/OSCC co-cultures. To this end, Cx43 expression and so gap junction formation can be further validated through transmission electron microscopy (TEM) with immunogold labeling of Cx43 (83). Moreover, GJIC can be further examined by other experiments, such as the widely used scrape loading and dye transfer assay (SL/DT) (75). In this approach, a scratch is made in a monolayer of adherent cells. Due to the mechanical perturbation of the cell membrane, a gap junction permeable tracer, such as Lucifer Yellow, can be inserted into the cells along the scrape. Normal membrane permeability will be restored, causing entrapment of this tracer in the cytoplasm. Over time, the tracer can transfer through the gap junctions to neighboring cells. In addition, the functionality of the formed gap junctions can further be validated through the use of gap junction blockers/inhibitors such as GAP27 or Cx43 silencing RNA (84). Herewith, no dye transfer should be observed in the used experiments.

Moreover, a limited number of biological replicates could be obtained during the 3D co-culture analysis and killing efficiency experiments. However, this number should increase in future research to validate our results. Additionally, the optimal DPSC/OSCC ratio should be determined to examine optimal cell death. Besides confluence and alamarBlue analysis, other experiments to assess cell death can strengthen our results. Viability/cytotoxicity of the DPSC/OSCC co-cultures can be evaluated through the LIVE/DEAD Viability/Cytotoxicity kit via FACS. Another experiment that is widely used to assess cell death after GCV administration is the 3-(4,5-Dimethylthiazol-2-yl)-2,5-diphenyltetrazolium bromide (MTT) assay (77, 78). In addition, cell death after GCV administration should be assessed in a 3D co-culture to give a better representation of the *in vivo* situation (74). The toxicity of high doses of GCV should be investigated and considered for future *in vivo* research to minimize side effects caused by prodrug administration. Furthermore, transduced DPSC killing efficiency should be examined with different OSCC cancer cell lines due to the variations in cell-intrinsic tumor cell properties which influence sensitivity to cell death (56).

In the future, *in vivo* research of our proposed therapy in a head and neck cancer rat model should be assessed. Our research group optimized this *in vivo* model by the administration of tobacco-derived carcinogen 4-nitroquinoline-1-oxide (4NQO) in the drinking water of rats. During *in vivo* studies, the optimal amount of HSV1-tk$^+$-DPSC, their persistence, and the number of therapy injection rounds should be assessed while non-invasively monitoring tumor volume and transduced DPSC cell death.

CONCLUSION

Our results indicate the successful transduction of all three DPSC donor cell lines with no adverse effects on DPSC marker expression. Furthermore, our data demonstrates functional gap junction formation in a DPSC/OSCC co-culture. HSV1-tk$^+$-DPSC killing efficiency was validated after six days with a GCV concentration as low as 0.1µM *in vitro*. In addition, seven days after GCV administration to *in vivo* injected transduced DPSC, cell viability diminished. Although further validation is needed, this project shows promising results of using HSV1-Tk expressing DPSC as therapeutic vehicles to eradicate OSCC.

REFERENCES

1. organization Wh. Cancer 2021 [Available from: https://www.who.int/news-room/fact-sheets/detail/cancer.
2. Hanahan D, Weinberg RA. The hallmarks of cancer. Cell. 2000;100(1):57-70.
3. Hanahan D, Weinberg RA. Hallmarks of cancer: the next generation. Cell. 2011;144(5):646-74.
4. Senga SS, Grose RP. Hallmarks of cancer-the new testament. Open Biol. 2021;11(1):200358.
5. Ferlay J, Colombet M, Soerjomataram I, Parkin DM, Pineros M, Znaor A, et al. Cancer statistics for the year 2020: An overview. Int J Cancer. 2021.
6. Johnson DE, Burtness B, Leemans CR, Lui VWY, Bauman JE, Grandis JR. Head and neck squamous cell carcinoma. Nat Rev Dis Primers. 2020;6(1):92.

7. Markopoulos AK. Current aspects on oral squamous cell carcinoma. Open Dent J. 2012;6:126-30.
8. Schiff BA. Oral Squamous Cell Carcinoma: MSD manual professional version; 2021 [Available from: https://www.msdmanuals.com/professional/ear,-nose,-and-throat-disorders/tumors-of-the-head-and-neck/oral-squamous-cell-carcinoma.
9. Zygogianni AG, Kyrgias G, Karakitsos P, Psyrri A, Kouvaris J, Kelekis N, et al. Oral squamous cell cancer: early detection and the role of alcohol and smoking. Head Neck Oncol. 2011;3:2.
10. Warnakulasuriya S, Sutherland G, Scully C. Tobacco, oral cancer, and treatment of dependence. Oral Oncol. 2005;41(3):244-60.
11. Ramqvist T, Dalianis T. An epidemic of oropharyngeal squamous cell carcinoma (OSCC) due to human papillomavirus (HPV) infection and aspects of treatment and prevention. Anticancer Res. 2011;31(5):1515-9.
12. society Ac. Treatment Options for Oral Cavity Cancer by Stage 2021 [Available from: https://www.cancer.org/cancer/oral-cavity-and-oropharyngeal-cancer/treating/by-stage.html.
13. Society TAC. Radiation Therapy for Oral Cavity and Oropharyngeal Cancer [Available from: https://www.cancer.org/cancer/oral-cavity-and-oropharyngeal-cancer/treating/radiation-therapy.html#written_by.
14. society Ac. Chemotherapy for Oral Cavity and Oropharyngeal Cancer 2021 [Available from: https://www.cancer.org/cancer/oral-cavity-and-oropharyngeal-cancer/treating/chemotherapy.html.
15. Cheng SC, Wu VW, Kwong DL, Ying MT. Assessment of post-radiotherapy salivary glands. Br J Radiol. 2011;84(1001):393-402.
16. Sayan M, Cassidy RJ, Switchenko JM, Kayode OA, Saba NF, Steuer CE, et al. Development of Late Toxicities in Patients with Oral Tongue Cancer Treated with Surgical Resection and Adjuvant Radiation Therapy. Front Oncol. 2016;6:272.
17. Chhatui B, Devleena, Roy S, Maji T, Lahiri D, Biswas J. Immunomodulated anterior chemotherapy followed by concurrent chemoradiotherapy in locally advanced tongue cancer: An Institutional experience. Indian J Med Paediatr Oncol. 2015;36(1):43-8.
18. Meng J, Gu QP, Meng QF, Zhang J, Li ZP, Si YM, et al. Efficacy of nimotuzumab combined with docetaxel-cisplatin-fluorouracil regimen in treatment of advanced oral carcinoma. Cell Biochem Biophys. 2014;68(1):181-4.
19. Chang PM, Lu HJ, Wang LW, Tai SK, Chen MH, Chu PY, et al. Effectiveness of incorporating cetuximab into docetaxel/cisplatin/fluorouracil induction chemotherapy and chemoradiotherapy for inoperable squamous cell carcinoma of the oral cavity: A phase II study. Head Neck. 2017;39(7):1333-42.
20. Sun W, Shi Q, Zhang H, Yang K, Ke Y, Wang Y, et al. Advances in the techniques and methodologies of cancer gene therapy. Discov Med. 2019;27(146):45-55.
21. High KA, Roncarolo MG. Gene Therapy. N Engl J Med. 2019;381(5):455-64.
22. Corban-Wilhelm H, Becker G, Bauder-Wust U, Greulich D, Debus J. Cytosine deaminase versus thymidine kinase: a comparison of the antitumor activity. Clin Exp Med. 2003;3(3):150-6.
23. Eissenberg LG, Rettig M, Dehdashti F, Piwnica-Worms D, DiPersio JF. Suicide genes: monitoring cells in patients with a safety switch. Front Pharmacol. 2014;5:241.
24. Finocchiaro LM, Bumaschny VF, Karara AL, Fiszman GL, Casais CC, Glikin GC. Herpes simplex virus thymidine kinase/ganciclovir system in multicellular tumor spheroids. Cancer Gene Ther. 2004;11(5):333-45.
25. Karjoo Z, Chen X, Hatefi A. Progress and problems with the use of suicide genes for targeted cancer therapy. Adv Drug Deliv Rev. 2016;99(Pt A):113-28.
26. Ardiani A, Johnson AJ, Ruan H, Sanchez-Bonilla M, Serve K, Black ME. Enzymes to die for: exploiting nucleotide metabolizing enzymes for cancer gene therapy. Curr Gene Ther. 2012;12(2):77-91.
27. Gambhir SS, Bauer E, Black ME, Liang Q, Kokoris MS, Barrio JR, et al. A mutant herpes simplex virus type 1 thymidine kinase reporter gene shows improved sensitivity for imaging reporter gene expression with positron emission tomography. Proc Natl Acad Sci U S A. 2000;97(6):2785-90.

28. Black ME, Kokoris MS, Sabo P. Herpes simplex virus-1 thymidine kinase mutants created by semi-random sequence mutagenesis improve prodrug-mediated tumor cell killing. Cancer Res. 2001;61(7):3022-6.
29. Faulds D, Heel RC. Ganciclovir. A review of its antiviral activity, pharmacokinetic properties and therapeutic efficacy in cytomegalovirus infections. Drugs. 1990;39(4):597-638.
30. Gambhir SS, Barrio JR, Wu L, Iyer M, Namavari M, Satyamurthy N, et al. Imaging of adenoviral-directed herpes simplex virus type 1 thymidine kinase reporter gene expression in mice with radiolabeled ganciclovir. J Nucl Med. 1998;39(11):2003-11.
31. Yaghoubi SS, Gambhir SS. Measuring herpes simplex virus thymidine kinase reporter gene expression in vitro. Nat Protoc. 2006;1(4):2137-42.
32. Penuelas I, Mazzolini G, Boan JF, Sangro B, Marti-Climent J, Ruiz M, et al. Positron emission tomography imaging of adenoviral-mediated transgene expression in liver cancer patients. Gastroenterology. 2005;128(7):1787-95.
33. Mese G, Richard G, White TW. Gap junctions: basic structure and function. J Invest Dermatol. 2007;127(11):2516-24.
34. Goodenough DA, Paul DL. Gap junctions. Cold Spring Harb Perspect Biol. 2009;1(1):a002576.
35. Weber PA, Chang HC, Spaeth KE, Nitsche JM, Nicholson BJ. The permeability of gap junction channels to probes of different size is dependent on connexin composition and permeant-pore affinities. Biophys J. 2004;87(2):958-73.
36. Rangel-Sosa MM, Aguilar-Cordova E, Rojas-Martinez A. Immunotherapy and gene therapy as novel treatments for cancer. Colomb Med (Cali). 2017;48(3):138-47.
37. Thomas CE, Ehrhardt A, Kay MA. Progress and problems with the use of viral vectors for gene therapy. Nat Rev Genet. 2003;4(5):346-58.
38. Kolios G, Moodley Y. Introduction to stem cells and regenerative medicine. Respiration. 2013;85(1):3-10.
39. Miura M, Gronthos S, Zhao M, Lu B, Fisher LW, Robey PG, et al. SHED: stem cells from human exfoliated deciduous teeth. Proc Natl Acad Sci U S A. 2003;100(10):5807-12.
40. Ledesma-Martinez E, Mendoza-Nunez VM, Santiago-Osorio E. Mesenchymal Stem Cells Derived from Dental Pulp: A Review. Stem Cells Int. 2016;2016:4709572.
41. Reagan MR, Kaplan DL. Concise review: Mesenchymal stem cell tumor-homing: detection methods in disease model systems. Stem Cells. 2011;29(6):920-7.
42. Yazid FB, Gnanasegaran N, Kunasekaran W, Govindasamy V, Musa S. Comparison of immunodulatory properties of dental pulp stem cells derived from healthy and inflamed teeth. Clin Oral Investig. 2014;18(9):2103-12.
43. Zhao Y, Wang L, Jin Y, Shi S. Fas ligand regulates the immunomodulatory properties of dental pulp stem cells. J Dent Res. 2012;91(10):948-54.
44. Shi S, Gronthos S. Perivascular niche of postnatal mesenchymal stem cells in human bone marrow and dental pulp. J Bone Miner Res. 2003;18(4):696-704.
45. Tirino V, Paino F, De Rosa A, Papaccio G. Identification, isolation, characterization, and banking of human dental pulp stem cells. Methods Mol Biol. 2012;879:443-63.
46. Merckx G, Lo Monaco M, Lambrichts I, Himmelreich U, Bronckaers A, Wolfs E. Safety and Homing of Human Dental Pulp Stromal Cells in Head and Neck Cancer. Stem Cell Rev Rep. 2021;17(5):1619-34.
47. Hilkens P, Gervois P, Fanton Y, Vanormelingen J, Martens W, Struys T, et al. Effect of isolation methodology on stem cell properties and multilineage differentiation potential of human dental pulp stem cells. Cell Tissue Res. 2013;353(1):65-78.
48. Tiscornia G, Singer O, Verma IM. Production and purification of lentiviral vectors. Nat Protoc. 2006;1(1):241-5.
49. Capote-Moreno A, Brabyn P, Munoz-Guerra MF, Sastre-Perez J, Escorial-Hernandez V, Rodriguez-Campo FJ, et al. Oral squamous cell carcinoma: epidemiological study and risk factor assessment based on a 39-year series. Int J Oral Maxillofac Surg. 2020;49(12):1525-34.

50. Hasegawa Y, Emi N, Shimokata K. Retroviral transfer of HSV1-TK gene into human lung cancer cell line. J Mol Med (Berl). 1995;73(3):107-12.
51. van Putten EH, Dirven CM, van den Bent MJ, Lamfers ML. Sitimagene ceradenovec: a gene-based drug for the treatment of operable high-grade glioma. Future Oncol. 2010;6(11):1691-710.
52. Tjuvajev JG, Chen SH, Joshi A, Joshi R, Guo ZS, Balatoni J, et al. Imaging adenoviral-mediated herpes virus thymidine kinase gene transfer and expression in vivo. Cancer Res. 1999;59(20):5186-93.
53. Yu D, Wang A, Huang H, Chen Y. PEG-PBLG nanoparticle-mediated HSV-TK/GCV gene therapy for oral squamous cell carcinoma. Nanomedicine (Lond). 2008;3(6):813-21.
54. Neves S, Faneca H, Bertin S, Konopka K, Duzgunes N, Pierrefite-Carle V, et al. Transferrin lipoplex-mediated suicide gene therapy of oral squamous cell carcinoma in an immunocompetent murine model and mechanisms involved in the antitumoral response. Cancer Gene Ther. 2009;16(1):91-101.
55. Thuenemann EC, Le DHT, Lomonossoff GP, Steinmetz NF. Bluetongue Virus Particles as Nanoreactors for Enzyme Delivery and Cancer Therapy. Mol Pharm. 2021;18(3):1150-6.
56. Matuskova M, Hlubinova K, Pastorakova A, Hunakova L, Altanerova V, Altaner C, et al. HSV-tk expressing mesenchymal stem cells exert bystander effect on human glioblastoma cells. Cancer Lett. 2010;290(1):58-67.
57. Kenarkoohi A, Bamdad T, Soleimani M, Soleimanjahi H, Fallah A, Falahi S. HSV-TK Expressing Mesenchymal Stem Cells Exert Inhibitory Effect on Cervical Cancer Model. Int J Mol Cell Med. 2020;9(2):146-54.
58. Leten C, Trekker J, Struys T, Roobrouck VD, Dresselaers T, Vande Velde G, et al. Monitoring the Bystander Killing Effect of Human Multipotent Stem Cells for Treatment of Malignant Brain Tumors. Stem Cells Int. 2016;2016:4095072.
59. Nakamizo A, Marini F, Amano T, Khan A, Studeny M, Gumin J, et al. Human bone marrow-derived mesenchymal stem cells in the treatment of gliomas. Cancer Res. 2005;65(8):3307-18.
60. Loebinger MR, Eddaoudi A, Davies D, Janes SM. Mesenchymal stem cell delivery of TRAIL can eliminate metastatic cancer. Cancer Res. 2009;69(10):4134-42.
61. Black ME, Newcomb TG, Wilson HM, Loeb LA. Creation of drug-specific herpes simplex virus type 1 thymidine kinase mutants for gene therapy. Proc Natl Acad Sci U S A. 1996;93(8):3525-9.
62. Li LQ, Shen F, Xu XY, Zhang H, Yang XF, Liu WG. Gene therapy with HSV1-sr39TK/GCV exhibits a stronger therapeutic efficacy than HSV1-TK/GCV in rat C6 glioma cells. ScientificWorldJournal. 2013;2013:951343.
63. Saito-Moriya R, Nakayama J, Kamiya G, Kitada N, Obata R, Maki SA, et al. How to Select Firefly Luciferin Analogues for In Vivo Imaging. Int J Mol Sci. 2021;22(4).
64. Pajarinen J, Lin TH, Goodman SB. Production of GFP and Luciferase-Expressing Reporter Macrophages for In Vivo Bioluminescence Imaging. Methods Mol Biol. 2018;1790:99-111.
65. Gerace D, Boulanger KR, Hyoje-Ryu Kenty J, Melton DA. Generation of a heterozygous GAPDH-Luciferase human ESC line (HVRDe008-A-1) for in vivo monitoring of stem cells and their differentiated progeny. Stem Cell Res. 2021;53:102371.
66. Amadeo F, Plagge A, Chacko A, Wilm B, Hanson V, Liptrott N, et al. Firefly luciferase offers superior performance to AkaLuc for tracking the fate of administered cell therapies. Eur J Nucl Med Mol Imaging. 2022;49(3):796-808.
67. Wolfs E, Verfaillie CM, Van Laere K, Deroose CM. Radiolabeling strategies for radionuclide imaging of stem cells. Stem Cell Rev Rep. 2015;11(2):254-74.
68. Zhang B, Metharom P, Jullie H, Ellem KA, Cleghorn G, West MJ, et al. The significance of controlled conditions in lentiviral vector titration and in the use of multiplicity of infection (MOI) for predicting gene transfer events. Genet Vaccines Ther. 2004;2(1):6.
69. Wang J, Dai Y, Huang Y, Chen X, Wang H, Hong Y, et al. All-trans retinoic acid restores gap junctional intercellular communication between oral cancer cells with upregulation of Cx32 and Cx43 expressions in vitro. Med Oral Patol Oral Cir Bucal. 2013;18(4):e569-77.

70. Brockmeyer P, Hemmerlein B, Jung K, Fialka F, Brodmann T, Gruber RM, et al. Connexin subtype expression during oral carcinogenesis: A pilot study in patients with oral squamous cell carcinoma. Mol Clin Oncol. 2016;4(2):298-302.
71. Brockmeyer P, Jung K, Perske C, Schliephake H, Hemmerlein B. Membrane connexin 43 acts as an independent prognostic marker in oral squamous cell carcinoma. Int J Oncol. 2014;45(1):273-81.
72. Zhurova M, Woods EJ, Acker JP. Intracellular ice formation in confluent monolayers of human dental stem cells and membrane damage. Cryobiology. 2010;61(1):133-41.
73. Luzuriaga J, Pineda JR, Irastorza I, Uribe-Etxebarria V, Garcia-Gallastegui P, Encinas JM, et al. BDNF and NT3 Reprogram Human Ectomesenchymal Dental Pulp Stem Cells to Neurogenic and Gliogenic Neural Crest Progenitors Cultured in Serum-Free Medium. Cell Physiol Biochem. 2019;52(6):1361-80.
74. Antoine EE, Vlachos PP, Rylander MN. Review of collagen I hydrogels for bioengineered tissue microenvironments: characterization of mechanics, structure, and transport. Tissue Eng Part B Rev. 2014;20(6):683-96.
75. Abbaci M, Barberi-Heyob M, Blondel W, Guillemin F, Didelon J. Advantages and limitations of commonly used methods to assay the molecular permeability of gap junctional intercellular communication. Biotechniques. 2008;45(1):33-52, 6-62.
76. Park JH, Kim KI, Lee KC, Lee YJ, Lee TS, Chung WS, et al. Assessment of alpha-fetoprotein targeted HSV1-tk expression in hepatocellular carcinoma with in vivo imaging. Cancer Biother Radiopharm. 2015;30(1):8-15.
77. Lin MH, Wu SY, Wang HE, Liu RS, Chen JC. (1)(1)(1)In-DOTA-Annexin V for imaging of apoptosis during HSV1-tk/GCV prodrug activation gene therapy in mice with NG4TL4 sarcoma. Appl Radiat Isot. 2016;108:1-7.
78. He XL, Guo XJ, Qian GS, He XH, Huang GJ, Chen WZ, et al. Killing effects of ganciclovir on human pulmonary adenocarcinoma cell A549 transduced with HSV1-TK gene in vitro and in vivo. Acta Pharmacol Sin. 2001;22(10):901-6.
79. Salzberger B, Bowden RA, Hackman RC, Davis C, Boeckh M. Neutropenia in allogeneic marrow transplant recipients receiving ganciclovir for prevention of cytomegalovirus disease: risk factors and outcome. Blood. 1997;90(6):2502-8.
80. Janoly-Dumenil A, Rouvet I, Bleyzac N, Bertrand Y, Aulagner G, Zabot MT. Effect of duration and intensity of ganciclovir exposure on lymphoblastoid cell toxicity. Antivir Chem Chemother. 2009;19(6):257-62.
81. Deng WP, Wu CC, Lee CC, Yang WK, Wang HE, Liu RS, et al. Serial in vivo imaging of the lung metastases model and gene therapy using HSV1-tk and ganciclovir. J Nucl Med. 2006;47(5):877-84.
82. Hsieh YJ, Chen FD, Ke CC, Wang HE, Huang CJ, Hou MF, et al. The EIIAPA chimeric promoter for tumor specific gene therapy of hepatoma. Mol Imaging Biol. 2012;14(4):452-61.
83. Norris RP. Transfer of mitochondria and endosomes between cells by gap junction internalization. Traffic. 2021;22(6):174-9.
84. Manjarrez-Marmolejo J, Franco-Perez J. Gap Junction Blockers: An Overview of their Effects on Induced Seizures in Animal Models. Curr Neuropharmacol. 2016;14(7):759-71.

Acknowledgements – I want to especially thank Prof. dr. Wolfs and Miss Van den Bosch Jolien for granting me with the opportunity to complete my senior internship on this interesting topic that is close to my heart. I would like to thank them for sharing their knowledge and believing in me. My sincere appreciation goes towards Miss Van den Bosch Jolien, my daily supervisor, for her outstanding guidance throughout my senior internship, her never-ending enthusiasm and her trust in me. Furthermore, I would like to express my gratitude towards all the members of the FIERCE and LISSA research group for their help whenever needed and their pleasant conversations. They made me feel part of their team, for which I am grateful. Moreover, I am thankful for my fellow students for their support, interesting talks, confidence in me and their unconditional friendship. Finally my unlimited gratitude goes to my family, boyfriend and best friend for always believing in me, for all the talks, support and advice they granted me, for being proud of me and for the endless candles they burnt for good luck.

Author contributions – Prof. dr. Esther Wolfs conceived and designed this project. Fieten S. and Van den Bosch J. performed experiments and data analysis. Lentiviral transduction of DPSC was performed by Van den Bosch J. where Fieten S. followed along the process. Bex P. and Vella Y. provided assistance with cell-patching for the Lucifer Yellow dye transfer assay. Fieten S. wrote the paper. Van den Bosch J. carefully edited the manuscript.

Supplementary information

Table S.1 – **Abbreviation list**

(q)PCR	Quantitative polymerase chain reaction
[18F]FHBG	9-[4-[18F]fluoro-3-(hydroxymethyl)butyl]guanine
4NQO	4-nitroquinoline-1-oxide
5-FC	5-fluorocytosine
5-FU	5-fluorouracil
BLI	Bioluminescence imaging
CD	Cytosine deaminase
CD105	Endoglin
CD73	Ecto-5′-nucleotidase
CD90	Cluster of Differentiation 90
Cx43	Connexin 43
cycA	D-serine/alanine/glycine/:H(+)symporter
DAPI	4,6-diamidino-2- phenylindole
DPSC	Dental pulp stem cells
EF1α	Human elongation factor-1 alpha
FBS	Fetal bovine serum
Fluc	Firefly luciferase
GCV	Ganciclovir
GDEPT	Gene-directed enzyme prodrug therapy
GJIC	Gap junctional intercellular communication
HSV1-tk/HSV1-TK	Herpes simplex virus type 1 – thymidine kinase
ICC	Immunocytochemistry
IRES	Internal ribosome entry site
ISCT	International Society for Cellular Therapy
LY	Lucifer Yellow
MEM	Minimum Essential Medium Eagle
MOI	Multiplicity of infection
MSC	Mesenchymal stem cells
MTT	3-(4,5-Dimethylthiazol-2-yl)-2,5-diphenyltetrazolium bromide
ns	Not significant
OSCC	Oral squamous cell carcinoma
PET	Positron emission tomography
RLU	Relative light units
Rluc	Renilla luciferase
ROI	Regions of interest
S.E.M.	Standard error of the mean
SL/DT	Scrape loading and dye transfer assay
T2A	Peptide2A
TEM	Transmission electron microscopy
YWHAZ	Tyrosine 3-Monooxygenase/tryptophan 5-monooxygenase activation protein zeta
ZOL	Ziekenhuis Oost-Limburg
α-MEM	alpha modified Minimum Essential Medium

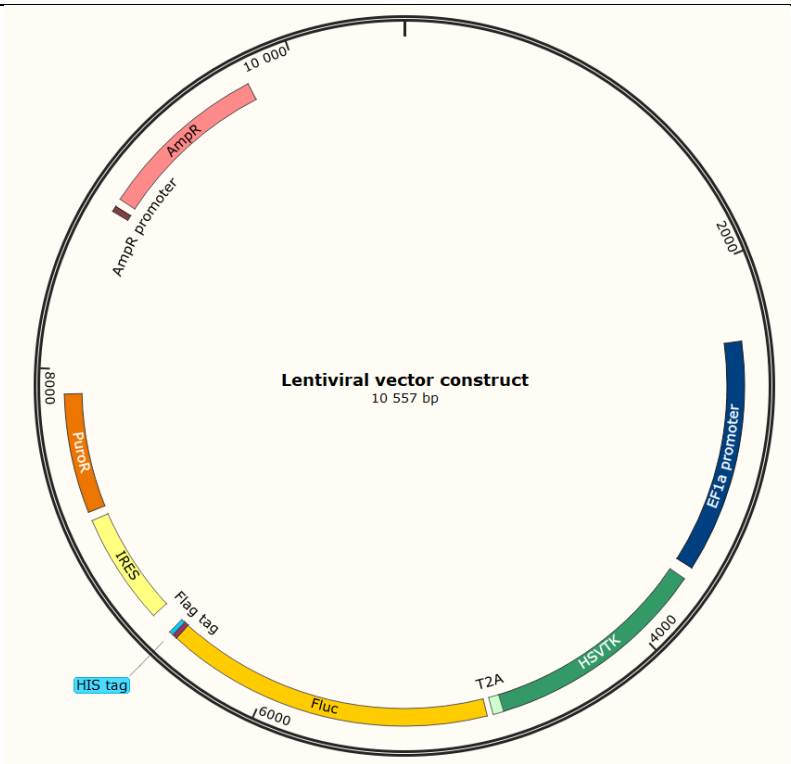

Figure S.1 - Lentiviral vector construct for HSV1-tk expression. The lentiviral vector construct encodes the human elongation factor-1 alpha (EF1α) promoter, HSV1-sr39tk, a peptide 2A (T2A) linker sequence, His-FLAG tagged firefly luciferase (Fluc), an internal ribosome entry site (IRES) and a puromycin resistance cassette. Ampicillin resistance is included in the vector construct for bacterial selection.
Figure created with SnapGene

Table S.2 – Primer pairs

Gene	Primer type	Sequence
HSV1-tk	Forward	5'- ACGTACCCGAGCCGATGACTTAC -3'
	Reverse	5'- TACCGCACCGTATTGGCAAGTAGC -3'
CD90	Forward	5'- AGAGACTTGGATGAGGAG -3'
	Reverse	5'- CTGAGAATGCTGGAGATG -3'
CD73	Forward	5'- CAGTACCAGGGCACTATCTGG -3'
	Reverse	5'- AGTGGCCCCTTTGCTTTAAT -3'
CD105	Forward	5'- CCACTAGCCAGGTCTCGAAG -3'
	Reverse	5'- GATGCAGGAAGACACTGCTG -3'

HSV1-tk: Herpes simples virus type 1-thymidine kinase; CD90: Cluster of Differentiation 90; CD73: Ecto-5'-nucleotidase; CD105: Endoglin

Table S.3 – Antibodies

Antibody	Type	Manufacturer	Dilution	REF
Anti-His-Tag antibody, Rabbit monoclonal	Primary	Sigma-Aldrich, St-Louis, MO, USA	1:200	SAB5600227
Monoclonal ANTI-FLAG® M2 antibody produced in mouse	Primary	Sigma-Aldrich, St-Louis, MO, USA	1:500	F1804
HSV-1 Thymidine Kinase (TK) Rabbit Antibody, affinity purified	Primary	Virusys corporation, Biozol, Eching, Germany	1:200	H1A316-100
Anti-Connexin 43 / GJA1 antibody - Intercellular Junction Marker	Primary	Abcam, Cambridge, United Kingdom	1:1000 (cells) 1:500 (hydrogels)	ab11370
Donkey anti-Mouse IgG (H+L) Highly Cross-Adsorbed Secondary Antibody, Alexa Fluor™ 555	Secondary	Invitrogen, Thermo Fisher Scientific, Geel, Belgium	1:250	A31570
Donkey anti-Rabbit IgG (H+L) Highly Cross-Adsorbed Secondary Antibody, Alexa Fluor™ 555	Secondary	Invitrogen, Thermo Fisher Scientific, Geel, Belgium	1:250	A31572

HSV1-tk: Herpes simplex virus type 1-thymidine kinase